Forward Dynamics for Gait Analysis as an Intermediate Step to Motion Prediction

J. Cuadrado, U. Lugris

Lab. Ingenieria Mecanica, Escuela Politecnica Superior
University of La Coruña
Ferrol, Spain
javicuad@cdf.udc.es, ulugris@udc.es

R. Pamies-Vila, J.M. Font-Llagunes

Dept. of Mech. Eng. and Biomedical Eng. Research Centre
Universitat Politecnica de Catalunya
Barcelona, Spain
rosa.pamies@upc.edu, josep.m.font@upc.es

Abstract—Human motion prediction through computational simulation can serve as a tool to anticipate the result of surgery or to help in the design of prosthetic/orthotic devices. The latter is the motivation in a project being run by the authors, devoted to the design of an active stance-control knee-ankle-foot orthosis (SCKAFO) as an assistive device for the gait of incomplete spinal cord injured (SCI) subjects. Optimization is a well-suited technique to tackle the human motion prediction problem, and several approaches have been proposed in the literature. However, no matter which is the used approach, the implementation of these methods represents a great challenge in terms of both convergence and efficiency. Therefore, the authors intend to firstly address the analysis of a certain measured motion through forward dynamics, which can be considered as an intermediate step towards the prediction problem, since it requires dynamical consistency too, but does not suffer from the same high amount of uncertainty. Consequently, a systematic study of the different alternatives to obtain, through forward dynamics, the drive efforts at joint level that produce a certain known motion is started in this paper. Three model-based control methods have been implemented for the gait of a healthy subject, and their performances have been compared.

Keywords—gait analysis; forward dynamics; motion simulation; model-based control

I. INTRODUCTION

Many spinal cord injured subjects with no ability to control their knee and ankle joints can walk with the help of assistive devices, such as crutches and orthoses. The knee–ankle–foot orthoses (KAFO) commonly used by these patients lock the knee joint flexion–extension in order to bear their weight during stance. The problem of locking the knee is that the hip must be lifted in order to leave enough clearance for the leg to complete the swing, thus leading to an energetically inefficient gait. There are several orthoses and knee articulation modules in the market which allow to unlock the knee flexion during leg swing to improve gait. However, they do not provide the necessary torque to perform the flexion–extension motion, and in many cases they require the patient to lock/unlock the knee manually at each step, by means of a remote control device. The development of an active KAFO [1, 2] with an actively controlled knee joint can greatly reduce the metabolic cost, which would encourage the patients to

choose walking instead of using wheelchairs, thus improving their rehabilitation.

Fig. 1. Authors' ongoing project: development of active SCKAFO.

The authors' ongoing project is devoted to the development of such an active stance-control knee-ankle-foot orthosis (SCKAFO) [3], shown in Fig. 1. The gait of patients wearing their passive orthoses is analyzed by means of an experimental setup for measuring gait data, which is fed into a multibody computational model that calculates the joint motor torques through inverse dynamics [4]. The obtained kinematic and kinetic information is useful for the design of the SCKAFO controllers. However, a most powerful tool would be that capable of answering the following question: how would this patient walk if he wore the SCKAFO we have developed with a certain design of the controller? Or, in other words, a tool capable of providing the patient's motion prediction. With such a tool, the SCKAFO controllers could be tuned once and again until a satisfactory behavior of the patient's computational model would be achieved in the simulation.

The problem of human motion prediction has been addressed in the literature, and is currently a topic of intensive research. Optimization has been the preferred technique, where the cost function is usually based on physiological criteria. Three main basic approaches have been used in the literature [5]:

a) To consider the parameters defining the motion as the design variables, obtaining the drive efforts that

originate the corresponding motion through inverse dynamics [6].

b) To consider the parameters defining the drive efforts as the design variables, obtaining the motion that results from the applied efforts through forward dynamics [7].

c) To consider both the parameters defining the motion and the drive efforts as the design variables, and including the relations among them (equations of motion) as constraints of the optimization problem [8].

However, no matter which is the used approach, the implementation of these methods represents a great challenge in terms of both convergence and efficiency.

On the other hand, the analysis of a real captured motion can be addressed by means of either inverse or forward dynamics [9]. While inverse dynamics looks at each discretized instant of time separately, forward dynamics implies by nature the dynamically consistent solution over the full period of motion, which is in better agreement with the operation rules of the musculoskeletal system. Therefore, the analysis of a certain measured motion through forward dynamics can be considered as an intermediate step towards the prediction problem, since it requires dynamical consistency too, but does not suffer from the same high amount of uncertainty.

Consequently, a systematic study of the different alternatives to obtain, through forward dynamics, the drive efforts at joint level (not muscular yet) that produce a certain known motion is started in this paper. The study focuses on gait, since this is the relevant motion for the authors' ongoing project, as explained before. The literature review showed that both control and optimization approaches have been used. Here, three model-based control methods have been implemented for a healthy subject and their performances have been compared.

The remaining of the paper is organized as follows. Section 2 describes the experiment, the multibody model of the healthy subject and the signal processing technique applied to the captured data. Section 3 gathers the multibody dynamics formulation. Section 4 explains the three methods that have been used to perform the forward dynamics analysis, shows the obtained results, and proceeds to their discussion. Section 5 draws the conclusions of the work and suggests the following research to be addressed.

II. EXPERIMENT AND MODEL

The subject selected to perform the experiment is a healthy adult male, 34 years old, mass 85 kg and height 1.82 m. He walks on a walkway featuring two embedded force plates (AMTI, AccuGait sampling at 100 Hz). The motion is captured by 12 optical infrared cameras (Natural Point, OptiTrack FLEX:V100 also sampling at 100 Hz) that compute the position of 37 optical markers.

The human body is modeled as a 3D multibody system formed by rigid bodies, as shown in Fig. 2. It consists of 18 anatomical segments: two hindfeet, two forefeet, two shanks, two thighs, pelvis, torso, neck, head, two arms, two forearms and two hands. The segments are linked by ideal spherical joints, thus defining a model with 57 degrees of freedom. The global axes are defined as follows: x axis in the antero–posterior direction, y axis in the medio–lateral direction, and z axis in the vertical direction. The computational model is defined with 228 mixed (natural + angular) coordinates. The subset of natural coordinates comprises the three Cartesian coordinates of 22 points, and the three Cartesian components of 36 unit vectors, thus making a total of 174 variables. The points correspond to the positions of all the spherical joints (white dots in Fig. 2), along with points of the five distal segments -head, hands and forefeet- (black dots in Fig. 2). Each one of the 18 bodies is defined by its proximal and distal points, plus two orthogonal unit vectors aligned at the antero–posterior and medio–lateral directions, respectively, when the model is in a standing posture. The remaining 54 variables are the 18 sets of 3 angles that define the orientation of each body with respect to the inertial frame.

The geometric and inertial parameters of the model are obtained, for the lower limbs, by applying correlation equations from a reduced set of measurements taken on the subject, following the procedures described in [10]. For the
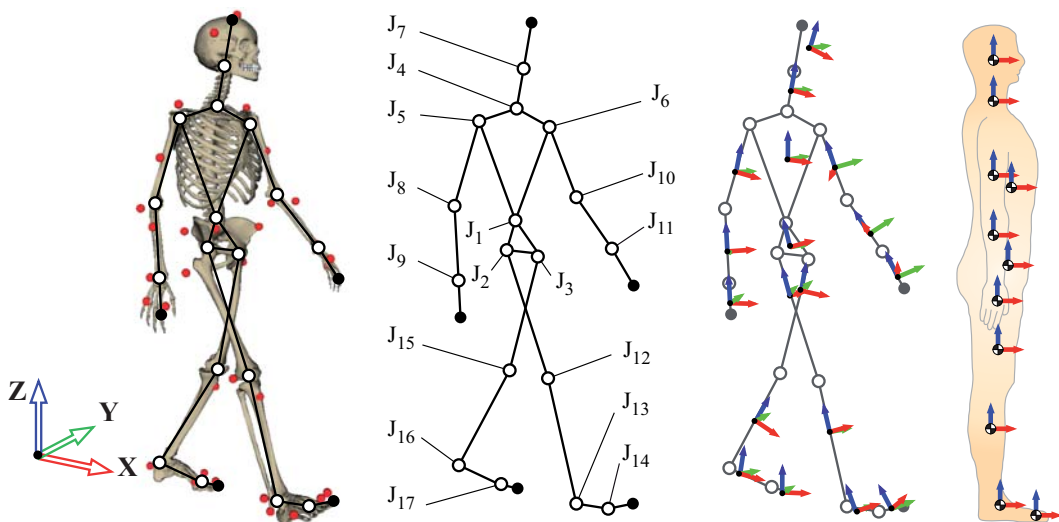

Fig. 2. (Color online) Human multibody model.

upper part of the body, data from standard tables [9] is scaled according to the mass and height of the subject. In order to adjust the total mass of the subject, a second scaling is applied to the inertial parameters of the upper part of the body.

The kinematic information of the motion is obtained from the trajectories of the 37 markers attached to the subject's body (red dots in Fig. 2), which are captured at 100 Hz frequency by means of the 12 infrared cameras. Position data are filtered using an algorithm based on Singular Spectrum Analysis (SSA) and the natural coordinates of the model are calculated using algebraic relations. Afterwards, a minimization procedure ensures the kinematic consistency of the natural coordinates. From that information, the histories of a set of 57 independent coordinates -as many as the system degrees of freedom- formed by the Cartesian coordinates of the position vector of the lumbar joint and the 18 x 3 angles that define the absolute orientation of each body, are kinematically obtained and approximated by using B-spline curves. Analytical differentiation yields the corresponding velocity and acceleration histories. More detail about the treatment of the captured data can be found in [4].

III. MULTIBODY FORMULATION

The dynamics of a multibody system can be described by the constrained Lagrangian equations,

$$\mathbf{M\ddot{q}} + \mathbf{\Phi_q^T \lambda} = \mathbf{Q}$$
$$\mathbf{\Phi} = \mathbf{0} \tag{1}$$

which constitute a set of differential-algebraic equations (DAE), where $\mathbf{M}$ is the positive semidefinite mass matrix, $\mathbf{\ddot{q}}$ the accelerations vector, $\mathbf{\Phi}$ the constraints vector, $\mathbf{\Phi_q}$ the Jacobian matrix of the constraints, $\mathbf{\lambda}$ the Lagrange multipliers vector, and $\mathbf{Q}$ the forces vector.

In this work, the formulation in minimum number of coordinates proposed in [11] and called matrix-R formulation has been used. The starting point is to establish the following relation between dependent $\mathbf{\dot{q}}$ and independent $\mathbf{\dot{z}}$ velocities:

$$\mathbf{\dot{q}} = \mathbf{R\dot{z}} \tag{2}$$

In the present case, vector $\mathbf{q}$ is formed by all the 228 problem variables, while vector $\mathbf{z}$ is formed by the subset of 57 independent coordinates (Cartesian coordinates of the position vector of the lumbar joint and orientation angles of all the anatomical segments) already mentioned in the previous section.

Relation (2) can always be found: each column of matrix $\mathbf{R}$ is nothing but the system velocities $\mathbf{\dot{q}}$ when a unit value is given to one of the independent velocities $\mathbf{\dot{z}}$ and the others are set to zero. The system velocity analysis can be carried out by means of the time derivative of the constraints equation, $\mathbf{\Phi_q \dot{q}} = \mathbf{0}$. Differentiating (2) with respect to time yields,

$$\mathbf{\ddot{q}} = \mathbf{R\ddot{z}} + \mathbf{\dot{R}\dot{z}} \tag{3}$$

where vector $\mathbf{\dot{R}\dot{z}}$ can be obtained by means of a system acceleration analysis with all the independent accelerations $\mathbf{\ddot{z}}$ set to zero. The system acceleration analysis can be carried out through the second time derivative of the constraints equation, $\mathbf{\Phi_q \ddot{q}} = -\mathbf{\dot{\Phi}_q \dot{q}}$.

Now, substituting (3) into (1), premultiplying by $\mathbf{R}^T$, and taking into account that $\mathbf{\Phi_q R} = \mathbf{0}$, the following system of ordinary differential equations (ODE) is achieved,

$$\mathbf{R^T M R \ddot{z}} = \mathbf{R^T} \left(\mathbf{Q} - \mathbf{M \dot{R} \dot{z}} \right) \tag{4}$$

or, in a more compact form,

$$\mathbf{\bar{M}\ddot{z}} = \mathbf{\bar{Q}} \tag{5}$$

where $\mathbf{\bar{M}}$ and $\mathbf{\bar{Q}}$ are, respectively, the mass matrix and force vector projected to the minimum set of coordinates $\mathbf{z}$.

Therefore, the result is that the DAE system (1) expressed in dependent coordinates $\mathbf{q}$ has been converted into the ODE system (5) expressed in independent coordinates $\mathbf{z}$.

In the present work, the ODE system (5) has been numerically integrated in time by means of the single step, fixed time step, trapezoidal rule.

IV. TESTS AND DISCUSSION

As explained in the Introduction, a systematic study of the different alternatives to obtain, through forward dynamics, the drive efforts at joint level that produce a certain known gait motion is started in this paper.

Initially, the gait of the healthy subject described at the beginning of Section 2 is captured with the infrared cameras, and the corresponding ground contact forces are measured through the forces plates. An inverse dynamics analysis (IDA) is then carried out to determine the reactions and joint torques that produced the motion. The measurements coming from the force plates are only used to overcome the reaction indeterminacy arising during the double-support phase: the measured reactions are corrected so that their force and moment resultants are coincident with those provided by the IDA, the discrepancy being split proportionally to their absolute values.

To provide a certain validation, Fig. 3 shows the net torques in the lower limb joints (sagittal plane) obtained from the IDA, and compares them with the average torque (dashed line) bounded by the standard deviation (grey area) presented by Winter in [12]. The recorded motion contains more than one cycle. It starts at the heel strike of the right foot (0% of gait cycle), includes the next heel strike of the same foot (100%), and finishes at the toe-off of the left foot belonging to the next cycle (approx. 116%).

In what follows, the pelvis is considered as the base body of the kinematic chain and, then, the reactions are the
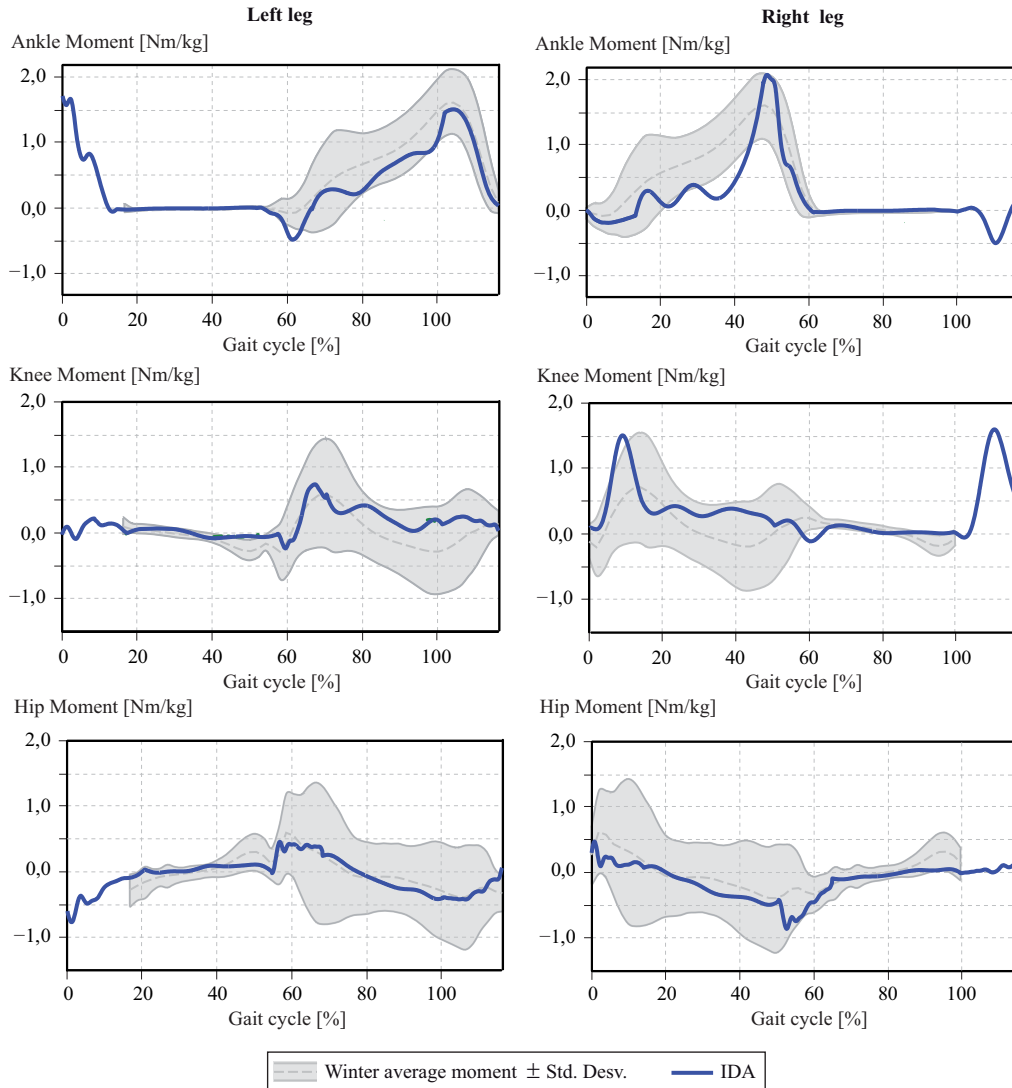
Left leg   **Right leg**

Fig. 3. (Color online) Comparison with Winter's results.

force and moment acting on the pelvis, while the drive torques are the absolute torques undergone by the remaining anatomical segments. Such results can be transformed, whenever necessary, to the reaction in the supporting foot (or to the reactions in the two supporting feet during double support, as explained above) and the actual drive torques at the joints.

Once the IDA has been carried out and the reaction force and moment have been determined along with the drive torques, the objective is to obtain the same reaction and drive torques by means of a forward dynamics analysis (FDA). For this purpose, the three following model-based control methods have been implemented:

a) The first method consists of using as inputs of the FDA the reaction and torques obtained from the IDA. Ideally, the solution should be coincident with the original captured motion but, as pointed out in the literature, it is not due to the unstable character of human gait and to the integration errors. Initially, a time step of 10 ms was adopted for the FDA, but the simulation was completely unstable. Then, the time-step size was reduced to 1 ms.

Since the IDA had been performed at 100 Hz, additional points had to be generated, which was straightforward as B-splines had been adjusted to the adquired motion, as explained in Section 2. Using the time step of 1 ms, the FDA was able to reproduce the motion until the 90% of the gait cycle and then drifted away, as illustrated in Fig. 4, where the ankle, knee and hip angles in the sagittal plane are plotted for both legs.

b) The second method consists of using as inputs of the FDA the reaction and torques obtained from the IDA (as in the first method), but includes a proportional-derivative (PD) control of reaction and torques so as to follow the measured motion and avoid instabilities. The reference signals of the controllers are the measured time evolution of the independent coordinates **z**, that is, the position of the lumbar joint and the three angles defining the absolute orientation of each segment. The error and the error time derivative of each controller have the following expressions:

$$e_i = z_i^{\text{ref}} - z_i \quad , \quad \dot{e}_i = \dot{z}_i^{\text{ref}} - \dot{z}_i \quad , \quad i = 1,...,57 \qquad (6)$$

Left leg

Ankle Joint Angle [deg]

Knee Joint Angle [deg]

Hip Joint Angle [deg]

Right leg

Ankle Joint Angle [deg]

Knee Joint Angle [deg]

Hip Joint Angle [deg]
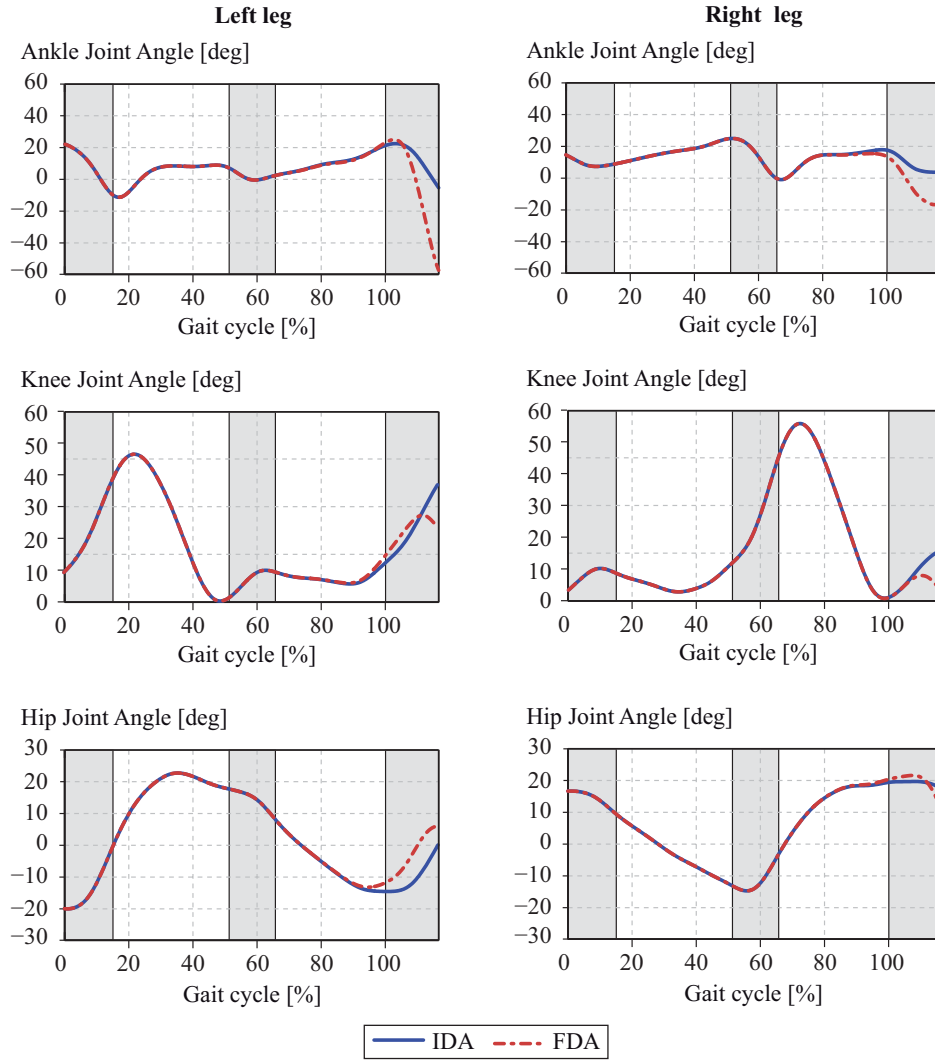

—— IDA   ‑‑‑‑ FDA

Fig. 4. (Color online) IDA results as inputs: FDA drifts away at 90% of gait cycle.

Therefore, an actuator associated to each independent coordinate is included for the FDA, its generalized force being,

$$f_i = k_{Pi}e_i + k_{Di}\dot{e}_i \quad , \quad i = 1,...,57 \qquad (7)$$

The gains k_{Pi} and k_{Di} for each actuator were adjusted by trial and error, and the results were shown to be quite sensitive to the values of the gains. Table 1 gathers the selected gain values. It can be seen that all the gains have been expressed as functions of two basic parameters, K_p and K_d. Moreover, the gains are proportional to the mass of the corresponding link, m_j.

As it happened for the first method, if a time step of 10 ms is used the simulation is completely unstable. However, using again a time step of 1 ms, the FDA was able to reproduce the entire motion. Fig. 5 shows the difference between the motion yielded by the FDA and the measured motion. The upper plot is devoted to the three Cartesian coordinates of the position vector of the lumbar joint (position errors are in the order of 10^{-7} m), while the

bottom plots refer to the thigh, shank, hindfoot and forefoot of the left and right legs, respectively (angular errors are in the order of 10^{-5} rad). Analogously, Fig. 6 shows the differences at force/torque level. In this case, errors in the reaction force at the lumbar joint are in the order of 10^{-2} N, while errors in the torques of the lower limbs are in the order of 10^{-4} Nm.

TABLE I.   SELECTED GAINS FOR THE PD CONTROLLERS

$K_p = 350$; $K_d = 1$		k_{Pi}/m_j	k_{Di}/m_j
Lumbar joint force	x	K_p	K_d
	y	$6K_p$	K_d
	z	$8K_p$	$8K_d$
Segment torques		$0.009K_p$	$0.003K_d$

c) The third method consists of using only, as input of the FDA, the actuation provided by the so-called computed torque control (CTC) [13]. The reference signals of the controllers are the same as those already explained for the previous method. In this case, the equations of motion (5) can be written as,
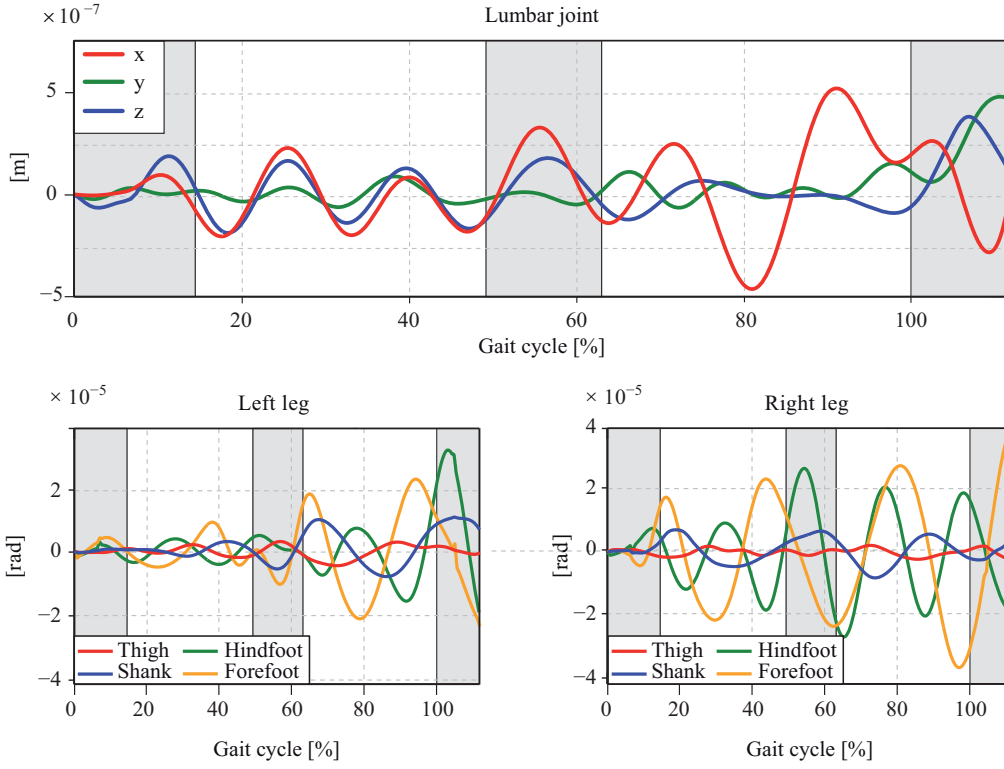
Fig. 5. (Color online) Differences between FDA and IDA results at position level (2nd method).
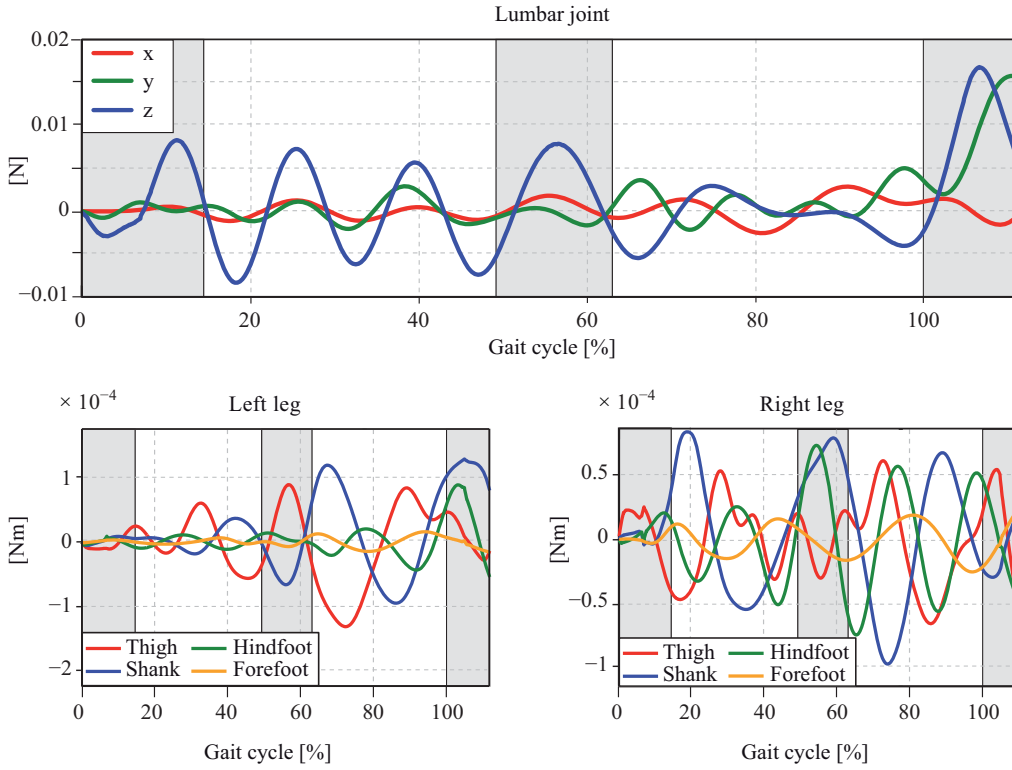

Fig. 6. (Color online) Differences between FDA and IDA results at force/torque level (2nd method).

$$\bar{\mathbf{M}}\ddot{\mathbf{z}} = \bar{\mathbf{Q}} + \bar{\mathbf{Q}}_{CTC} \qquad (8)$$

$$\bar{\mathbf{Q}}_{CTC} = \bar{\mathbf{M}}\left(\ddot{\mathbf{z}}^{ref} + \mathbf{c}_d\dot{\mathbf{e}} + \mathbf{c}_p\mathbf{e}\right) - \bar{\mathbf{Q}} \qquad (9)$$

where the vector of generalized forces due to the controllers takes the form,

being $\mathbf{c}_p$ and $\mathbf{c}_d$ diagonal matrices containing the gains associated to each independent coordinate z_i, $\mathbf{e}$ and $\dot{\mathbf{e}}$ the
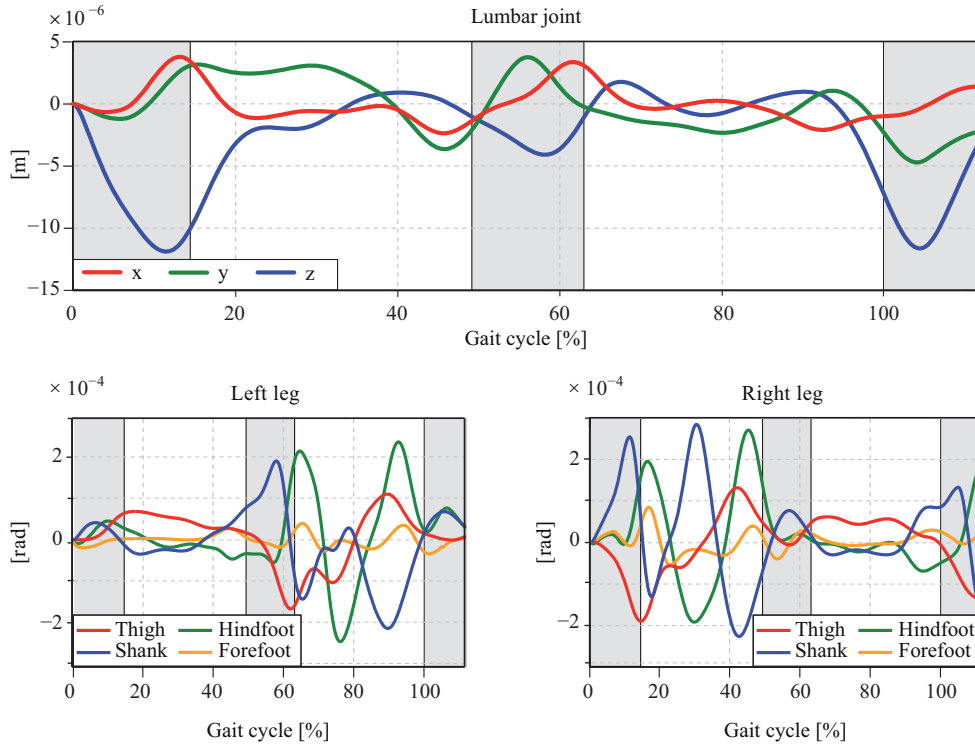
Fig. 7. (Color online) Differences between FDA and IDA results at position level (3rd method).
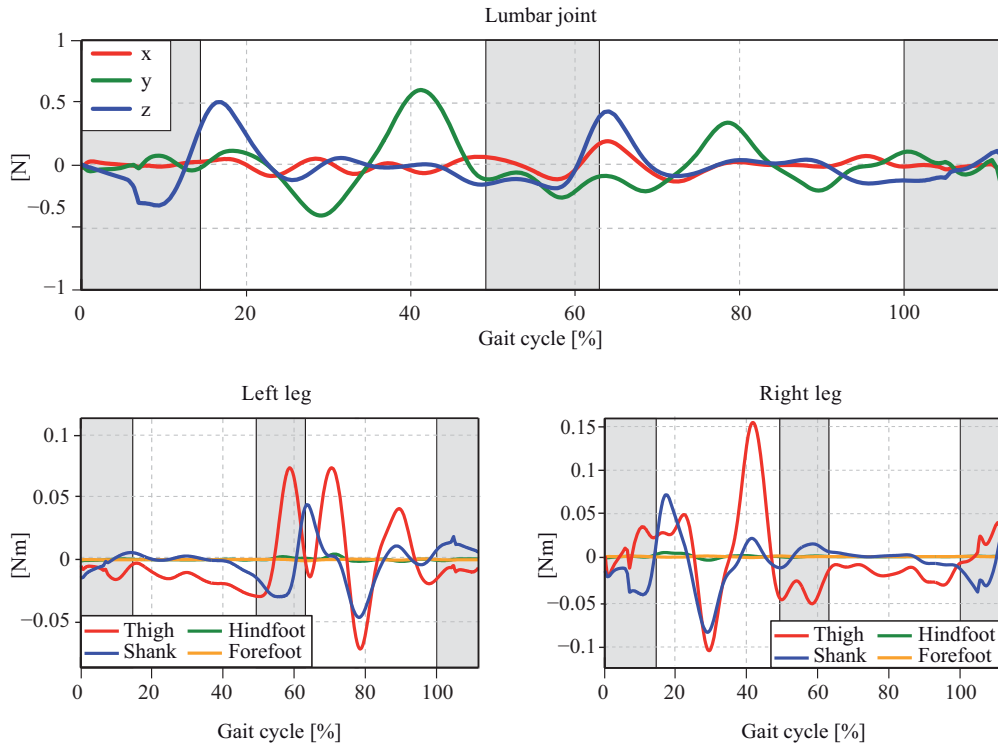

Fig. 8. (Color online) Differences between FDA and IDA results at force/torque level (3rd method).

vectors of error and error time derivative, respectively, as defined in (6), and $\ddot{\mathbf{z}}^{\text{ref}}$ the accelerations corresponding to the measured motion. As explained in [13], the error dynamics of this control method is represented by a system of second order differential equations, having $\mathbf{c}_{\text{p}}$ and $\mathbf{c}_{\text{d}}$ as coefficients of the proportional and first derivative terms, respectively. Therefore, if critical damping is desired, the following relation between the gains should be imposed,

$$\mathbf{c}_{\text{d}i} = 2\sqrt{\mathbf{c}_{\text{p}i}} \tag{10}$$

which means that only one of the two sets of coefficients must be adjusted. In this work, the $\mathbf{c}_p$ gains were considered as independent, while the $\mathbf{c}_d$ gains were obtained by application of (10).

Unlike the previous method, which required the particular tuning of each gain (as shown in Table 1), the CTC method allows giving the same value to all the $\mathbf{c}_{pi}$ elements, since each of them is affected by the corresponding generalized mass, as indicated in (9). Moreover, the method showed to be extremely robust, keeping the simulation stable for the wide range of gain values tested ($\mathbf{c}_{pi}$ was set to values of different magnitude orders, ranging from 10^{-1} to 10^5).

This time the controller was able to complete the FDA analysis with a time step of 10 ms, which further confirms the robustness of the method. The obtained results were quite accurate at position level, but showed relevant errors at force/torque level, i.e. the reaction and torques yielded by the FDA were not in good agreement with those provided by the IDA.

Using a time step of 1 ms, the FDA was carried out for the different values of $\mathbf{c}_{pi}$ indicated above. It was observed that the accuracy of the CTC method increases linearly with the value of $\mathbf{c}_{pi}$ (some noise appeared in the results for values of $\mathbf{c}_{pi}$ greater than 10^3). Setting $\mathbf{c}_{pi} = 10^3$, Fig. 7 shows the difference between the motion yielded by the FDA and the measured motion, while Fig. 8 shows the differences at force/torque level. The format of these figures is the same as that followed for the previous method in order to streamline comparison.

As it can be seen in the figures, position errors are in the order of 10^{-6} m and angular errors are in the order of 10^{-4} rad, while errors in the reaction force at the lumbar joint are in the order of 1 N and errors in the torques of the lower limbs are in the order of 10^{-1} Nm. Although this accuracy is lower than that provided by the previous method, the accuracy of the CTC method can be increased by simply increasing the value of $\mathbf{c}_{pi}$, as pointed out before.

V.   CONCLUSIONS AND FUTURE RESEARCH

Three methods have been tested in this paper to obtain, through forward dynamics, the drive efforts at joint level that produce a certain known gait motion. The first one consists of using as inputs of the forward dynamics analysis (FDA) the reaction and torques obtained from a previous inverse dynamics analysis (IDA). This method is not able to reproduce the motion due to the integration errors and the unstable character of human gait, which make the simulation drift. The second method adds a PD controller to the IDA reaction and torques, allowing to simulate the complete motion after a careful tuning of the PD gains. The last method does not require the IDA results, but implements a computed torque controller

instead. In this case, the parameters to be tuned are reduced to one single gain, and the method is robust with respect to both the gain and the time step values, providing higher accuracy for increasing gain values. Therefore, it is perceived as an excellent method for the pursued objective.

The next steps in this research, which has the final objective of developing motion prediction methods, will be oriented in two directions. On the one hand, control-based methods should be tested for the case of including foot-ground contact models in the simulation. On the other hand, optimization-based methods, in which the parameterized input forces are the design variables and the measured motion is the cost function, should be tested in order to get experience for the motion prediction challenge.

REFERENCES

[1]   A.M. Dollar and H. Herr, "Lower extremity exoskeletons and active orthoses: Challenges and state–of–the–art," IEEE Transactions on Robotics, vol. 24, no. 1, pp. 144–158, 2008.

[2]   T. Yakimovich, E.D. Lemaire, and J. Kofman, "Engineering design review of stance–control knee–ankle–foot orthoses." Journal of Rehabilitation Research and Development, vol. 46, no. 2, p. 257, 2009.

[3]   J.M. Font-Llagunes, R. Pamies-Vila, F.J. Alonso, U. Lugris, "Simulation and design of an active orthosis for an incomplete spinal cord injured subject," IUTAM Symposium on Human Body Dynamics: From Multibody Systems to Biomechanics, Procedia IUTAM, vol. 2, pp. 68-81, Waterloo, Canada, June 5-8, 2011.

[4]   U. Lugris, J. Carlin, A. Luaces, J. Cuadrado, "Gait analysis system for spinal cord injured subjects assited by active orthoses and crutches," Journal of Multi-body Dynamics, in press.

[5]   Y. Xiang, J.S. Arora, K. Abdel-Malek, "Physics-based modeling and simulation of human walking: a review of optimization-based and other approaches," Structural and Multidisciplinary Optimization, vol. 42, pp. 1-23, 2010.

[6]   L. Ren, R.K. Jones, D. Howard, "Predictive modelling of human walking over a complete gait cycle," Journal of Biomechanics, vol. 40, pp. 1567-1574, 2007.

[7]   F.C. Anderson, M.G. Pandy, "Dynamic optimization of human walking," Journal of Biomechanical Engineering, vol. 123, pp. 381-390, 2001.

[8]   Y. Xiang, J.S. Arora, K. Abdel-Malek, "Hybrid predictive dynamics: a new approach to simulate human motion," Multibody System Dynamics, vol. 28, no. 3, pp. 199-224, 2012.

[9]   J.A.C. Ambrosio, A. Kecskemethy, "Multibody dynamics of biomechanical models for human motion via optimization," Multibody Dynamics – Computational Methods and Applications, J.C. Garcia Orden, J.M. Goicolea, J. Cuadrado, Eds. Dordrecht: Springer, 2007, pp. 245-272.

[10] C.L. Vaughan, B.L. Davis, J.C. O'Connor, Dynamics of Human Gait, 2nd ed. Cape Town: Kiboho Publishers, 1999.

[11] J. Garcia de Jalon, E. Bayo, Kinematic and Dynamic Simulation of Multibody Systems. New York: Springer-Verlag, 1994.

[12] D.A. Winter, The Biomechanics and Motor Control of Human Gait: Normal, Elderly and Pathological. Waterloo: University of Waterloo Press, 1991.

[13] K.C. Gupta, Mechanics and Control of Robots. New York: Springer-Verlag, 1997.

ANSWERS TO REVIEWERS

Reviewer 1

The main contribution of the paper is an experimental comparison of three known optimization methods based on real motion capture data. These methods address the problem of forward human gait analysis. Pros and cons of each method have been reviewed and a quantitative comparison focusing on results' precision against real captured data has been provided. The paper is of interest to those working in the area of bio-mechanics, and hence, I recommend it for presentation in the conference.

Please clarify on how have you computed the geometric and dynamic parameters of the model.

Answers to reviewer 1

The paragraph referred to geometric and inertial parameters has been substituted by the following, where a couple of references have been added to clarify the way they have been obtained:

The geometric and inertial parameters of the model are obtained, for the lower limbs, by applying correlation equations from a reduced set of measurements taken on the subject, following the procedures described in [10]. For the upper part of the body, data from standard tables [9] is scaled according to the mass and height of the subject. In order to adjust the total mass of the subject, a second scaling is applied to the inertial parameters of the upper part of the body.

Reviewer 3

1. Before Section 3: Some plots on 1 or 2 of the 57 motion variables with their time-derivatives would be helpful for the readers to understand about what type of inputs are fed to IDA.

2. Equation (2) appears to be similar to some of the orthogonal based velocity transformations. See for example, Shah, et al., "Modular framework for dynamic modelling and analyses of legged robots," Int. J. of Mechanism and Machine Th., V. 49, pp. 234-255. Please refer 1-2 such publications.
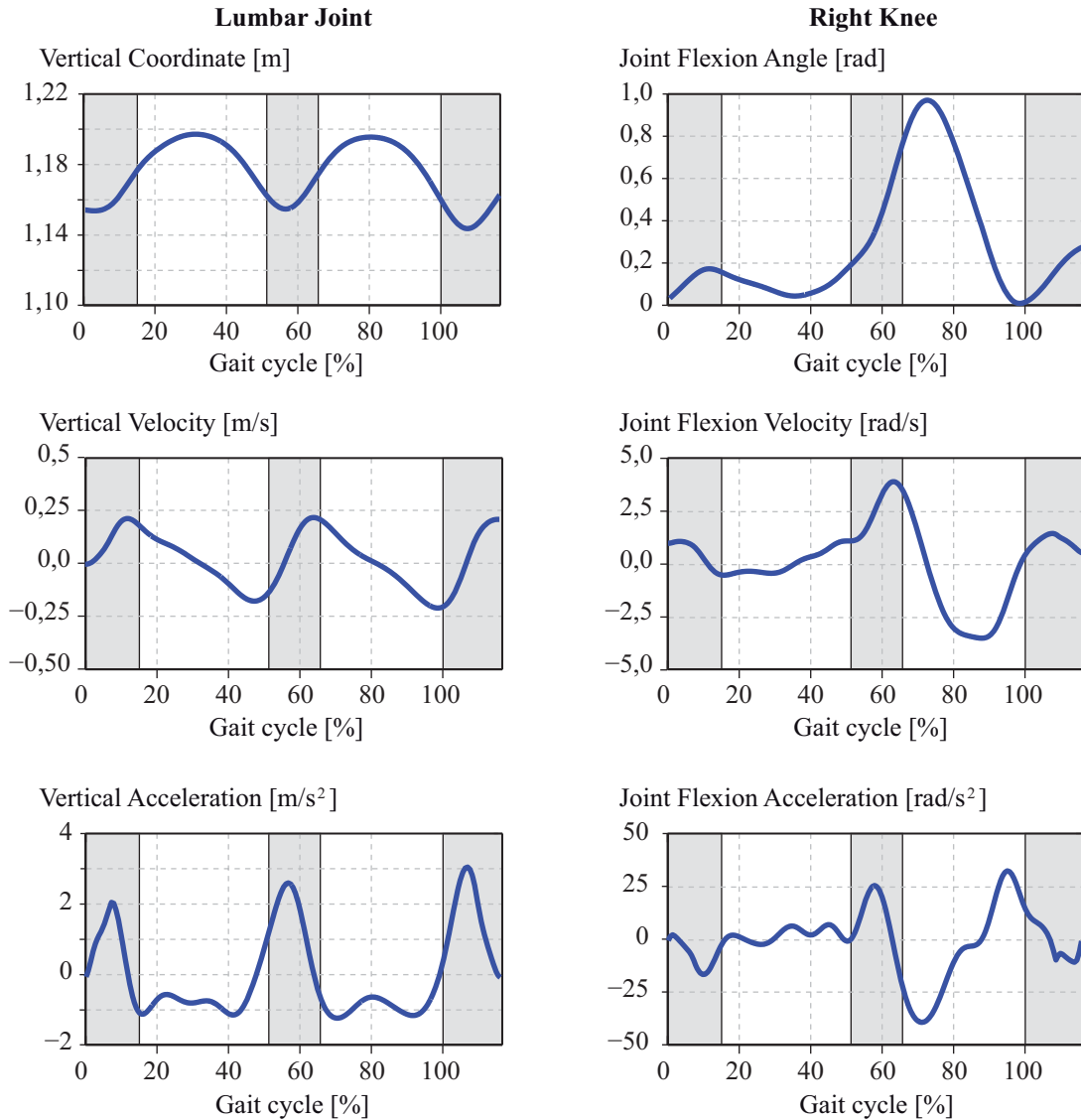
3. After figure 3: Can some plots on the errors be given on the IDA based motion vs. the real motion?

4. "Integration errors" mentioned after figure 3 is not the real cause of instability. It is more so due to zero eigen-value problem as mentioned in Shah, et al. (2013), "Dynamics of Tree-type Robotic Systems," Springer 2013.

5. After eq. (7): How the gains were found? Are there any interpretations for these gain values?

Answers to reviewer 3

1. The next figure shows, as examples, two motion variables (along with their two first derivatives) out of the 57 that are fed to IDA: they are the vertical coordinate of the lumbar joint and the knee flexion angle.

Lumbar Joint

Vertical Coordinate [m]

Right Knee

Joint Flexion Angle [rad]

Vertical Velocity [m/s]

Joint Flexion Velocity [rad/s]

Vertical Acceleration [m/s^2]

Joint Flexion Acceleration [rad/s^2]

Unfortunately, such plots cannot be included in the paper since it exactly fits in the eight pages allowed, so there is no space for more material. However, in Fig. 4 the histories of flexion angles for hips, knees and ankles are represented.

2. As the reviewer points out, the matrix-R formulation used in the paper is based on a velocity transformation which relates the minimun number of coordinates with a set of dependent coordinates, the relating matrix being the orthogonal complement of the constraints Jacobian, which therefore eliminates the Lagrange multipliers from the equations of motion. This formulation can be seen as the general case of the natural orthogonal complement (NOC) formulation developed for serial robots, where the joint coordinates are related to the twists of all the bodies. Moreover, a particular case of the NOC formulation is the decoupled natural orthogonal complement (DeNOC) formulation, where the relating matrix can be expressed as the product of a matrix

which contains the robot topology and a diagonal matrix, thus enabling recursivity in the process of obtaining the inertia matrix and force vector.

Again, it would be nice to include that kind of explanations in the paper, but space limitation makes it impossible.

3. The next figure shows, as example, the difference between raw and processed motion for two coordinates: the vertical coordinates of the lumbar joint and the right ankle joint. Differences are due to filtering and imposition of kinematic consistency.

Lumbar Joint   **Right Ankle Joint**
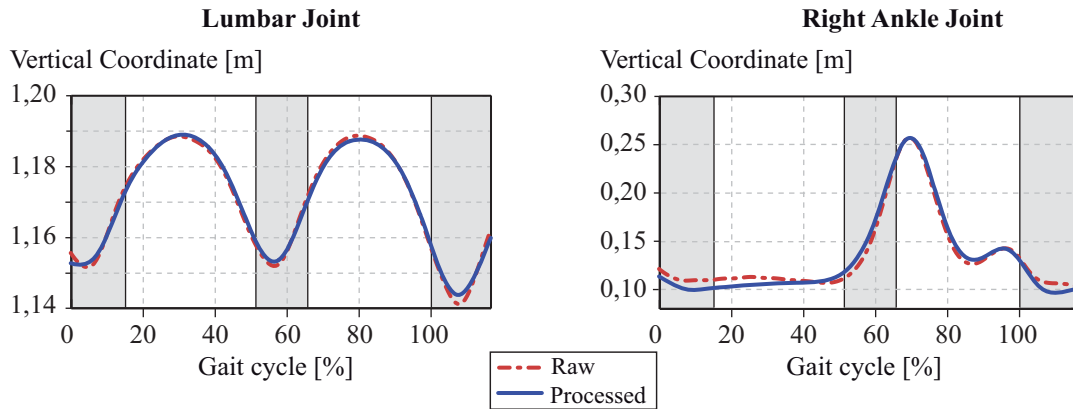
Once more, these plots cannot be included in the paper due to space limitations.

4. As the reviewer points out, the system is unstable and this is the cause of the drift. However, responsibility of the integrator is found in the fact that all numerical integrators provide the solution with an error, which makes that under a certain actuation the system doesn't move in the exact way. Consequently, although the drive forces obtained from inverse dynamics for a certain motion are exact, when they are input to a forward dynamics simulation, a discrete approach is followed, which means that the forces are considered at certain instants of time and, from one time to the next one, the system motion develops as decided by the integrator. Therefore, in the next instant of time, the system is not where it should be, due to the integrator error, and a new value of correct force is applied on it, but correct if the system was in the correct place, which is not the case.

The mentioned behavior is confirmed in the paper when the time-step size of integration is changed. The motion of the system is better reproduced as the time step is reduced, since the integrator error also decreases. In the limit, if the time step tended to zero, the integrator would have no error, and the motion would be perfectly reproduced (no drift would appear).

To emphasize that the mechanical cause of the drift is the instability of the system, while the mathematical one is the inaccuracy of the integrator, the first reason has been written before the second one in the paper.

5. As indicated just after eq. (7), the gains were adjusted by trial and error. As shown in Table 1, several measures were adopted to simplify the problem: a) two parameters were adopted, K_p and K_d, upon which all the gains were made dependent; b) only four different categories were considered, the three linear actuators (force at lumbar joint)

and the rotational actuators (torques at all the body segments), which means that only eight values (proportional and derivative gains for each of the four categories) had to be adjusted; c) proportionality to the corresponding link mass was also considered.

Regarding the physical meaning, the error is usually seen as the motion of a vibratory system, where the proportional gain plays the role of stiffness, the derivative gain the role of damping, and the integral gain the role of inertia.

Finally, acknowledgment is given to reviewer 3, since proposed reference S.V. Shah, S.K. Saha, J.K. Dutt, Modular framework for dynamic modeling and analyses of legged robots, Mechanism and Machine Theory, vol. 49, pp. 234-255, 2012, has resulted highly useful, since it addresses the same problem dealt with in our current research for humans, but for legged robots instead. We feel that such a reference as well as the book also proposed by the reviewer (Dynamics of Tree-type Robotic Systems), are to be really helpful in the forthcoming steps of our research.